34th Annual International Conference of the IEEE EMBS
San Diego, California USA, 28 August - 1 September, 2012

Predicting Failure in Soft Tissue Phantoms via Modeling of Non-Predetermined Tear Progression

Matthew Oldfield, Daniele Dini and Ferdinando Rodriguez y Baena

Abstract— **The advantageous, curved trajectory of bevel-tipped devices in soft tissue is a function of the interplay between material deformation, contact interactions and material failure. Highly detailed modeling of tool-tissue interactions is therefore vital in optimising performance and design. At high resolution, discontinuous failure of soft tissue phantoms has not been demonstrated. An iterative procedure, making incremental additions to the failure path in an otherwise continuous finite element mesh, is presented to achieve this goal. The procedure's efficacy was demonstrated in two materials including a soft tissue phantom. Failure path is shown to respond well to different and evolving shear and normal stress states. The iterative procedure would thus be ideal for analysing and optimising complex tool-tissue interactions, for instance in needle steering systems, where the path taken by the needle also depends on the progression of a tear which develops ahead of the tip during the insertion process. With the method presented here, this behaviour could be modeled and analysed at an unprecedented resolution.**

I. INTRODUCTION

With the continuing development of minimally-invasive and robotically-assisted surgery, the controlled insertion of needles and catheters has become a source of interest. It is well established that with the correct shaft and tip characteristics, needles can be pushed along curved trajectories. Benefits of these types of device are increased flexibility in targeting e.g. lesions and the possibility to access multiple locations from a single insertion point.

Bevel-tipped needles [1], [2] and flexible shaft manipulation [3] have been used as a means of generating curved trajectories within soft tissue. Using the principle of a bevel-tip to generate lateral forces, an alternative device has been developed using multiple, interlocked segments. A 'programmable bevel' concept that relates the relative offset of the leading probe segment to the radius of curvature in soft tissue phantoms has been demonstrated by [4] and [5] in conjunction with the current authors. For this device, with its novel actuation mechanism, a detailed understanding of probe-tissue interactions is required. High resolution numerical models offer the opportunity to change model parameters and obtain diagnostic output. Detailed finite element models, also capable of demonstrating cutting of soft tissue phantoms, are therefore ideal for optimising the performance of bevel-tipped devices.

All authors are with the Department of Mechanical Engineering, Imperial College, Exhibition Road, London, SW7 2AZ, United Kingdom. e-mails: m.oldfield@imperial.ac.uk; d.dini@imperial.ac.uk; f.rodriguez@imperial.ac.uk.

The research leading to these results has received funding from the European Research Council under the European Union's Seventh Framework Programme (FP7/2007-2013) / ERC grant agreement n° 258642-STING

Modeling cutting and damage in tool-tissue interactions remains a challenge at high resolutions. Gokgol et al. [6] investigates the fracture toughness of liver for use with finite element models and, in [7], cohesion is investigated as an implementation of cutting in biological tissue. Adaptive mesh and cohesive zone approaches are applied in [8] and [9] respectively for crack propagation. By combining experiments establishing the strain energy release rate for soft tissue phantoms with a cohesive approach, [10] has shown how high resolution models with cutting can be achieved for needle insertions. The limitation here was the predefined failure path of the gelatin tissue phantom. Complex interactions seen with bevel-tipped devices must be modeled without an assumed material failure trajectory.

This paper outlines an approach for finite element modeling of non-predetermined cohesive failure in soft tissue phantoms. At a resolution high enough for physical insight, a procedure is presented that uses commercial software to project a failure path. This procedure addresses complexities introduced by substantial deformations and the subsequent need to implement an explicit solution procedure.

In Section II a method for using cohesion in finite element models with unspecified failure paths is presented. Sections III and IV describe tests and results used to validate this approach, including with a gelatin soft tissue phantom material. Section V provides a discussion of these results with conclusions as to the suitability of the approach, and its use in optimisation processes is outlined in Section VI.

II. THEORY

In this section the background of a finite element procedure for non-predetermined failure is presented that is suitable for use in soft tissue phantoms. Initially the material parameter, known as the strain energy release rate is introduced. Subsequent implementation of the strain energy release rate within the finite element framework is possible through the use of cohesive elements. Iterative use of a model with progressive cohesive failure is then described – allowing the crucial progression to a non-predetermined failure path.

A. Strain Energy Release Rate

The propagation of material failure on an energetic level leads to the definition of the strain energy release rate. This parameter represents the energy required to form a crack of a given surface area in a material, and results from all of the linear and nonlinear processes contributing to crack growth. Assuming a linear elastic material, the energy balance during crack propagation is:

$$W_{ext} = W_f + W_\varepsilon + W_{Gc} \tag{1}$$

where W_{ext} is the external work on the system; W_f is the work done in overcoming friction at any contacting surfaces; W_ε is the work converted to stored strain energy and W_{Gc} is the energy required to create a crack of given area. Strain energy release rate of a material for a given failure mechanism is then calculated as:

$$G_c = \frac{W_{Gc}}{A} \tag{2}$$

where G_c is the strain energy release rate and A is the area of the crack. Further details of how this energy balance can be used to establish the strain energy release rate of gelatin are given in [10].

B. Cohesive Elements

Once a value for the strain energy release rate of a material is established, it is implemented in the finite element method using cohesive elements. Here, the commercial software ABAQUS was used, with further details in [11]. Cohesive elements use a bilinear traction-separation relationship across an interface between continuum elements. The cohesive elements behave elastically until a yielding traction or separation is reached. As the separation continues to increase, the traction then decreases until it reaches zero. At this point, the cohesive element fails and is removed from the simulation [10]. The area under the traction-separation curve represents the strain energy release rate of the cohesive material.

C. Iterative Method

To implement cohesive elements into a non-predetermined crack propagation procedure, an iterative method was used. Starting with a continuous mesh, the simulation advanced until a trigger point, representing a condition for crack propagation, was met. Upon triggering, the stress state of the model was evaluated at the current crack tip and the most likely direction of crack propagation was established.

From the existing crack tip, a cohesive element was then inserted in the projected crack direction. This process resulted in a new crack tip at the termination of the layer of cohesive elements representing the evolving failure path. With this evolved topology, the simulation restarted and repeated the procedure – shown in Fig. 1.

Two criteria were used in establishing the likely crack projection. Initially, from a patch of elements surrounding the crack tip (Fig. 2), the normal stress, σ_{norm}, and the strain energy density, SED, were interpolated at n radii, r. The feasible projection angles, θ_{Range}, were fixed according to the limits of crack kinking due to pure shear in [12]. Within this range, the angles, $\theta_{norm,n}$, at which σ_{norm}, was maximum and SED was minimum, $\theta_{SED,n}$, were then determined.

$$\theta_{norm,n} = \underset{\theta \in \theta_{Range}}{\operatorname{argmax}} \left(\sigma_{norm}(r_n, \theta)\right) \tag{3}$$

$$\theta_{SED,n} = \underset{\theta \in \theta_{Range}}{\operatorname{argmin}} \left(SED(r_n, \theta)\right) \tag{4}$$

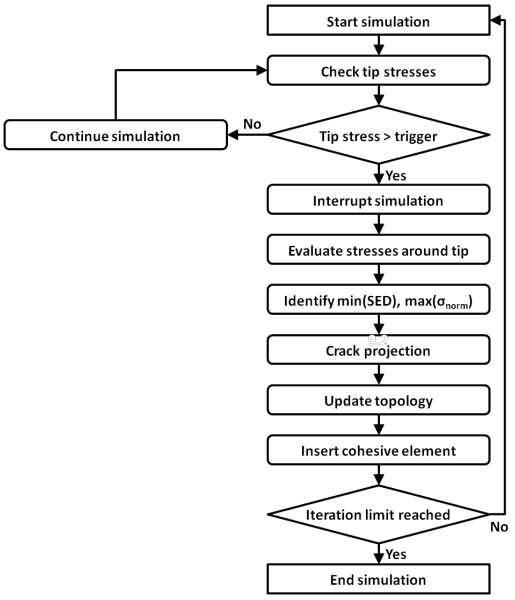

Fig. 1. Flowchart demonstrating the key steps in the iterative procedure to determine failure path

In both cases, to improve stability, only local maxima and minima were considered. Crack propagation direction, θ_P, was then taken as the mean of the sets of projections calculated using both methods:

$$\theta_P = \text{mean}\left\{\theta_{norm,1}, \ldots, \theta_{norm,n}, \theta_{SED,1}, \ldots, \theta_{SED,n}\right\} \tag{5}$$

which was then implemented as part of the iterative process of Fig. 1.

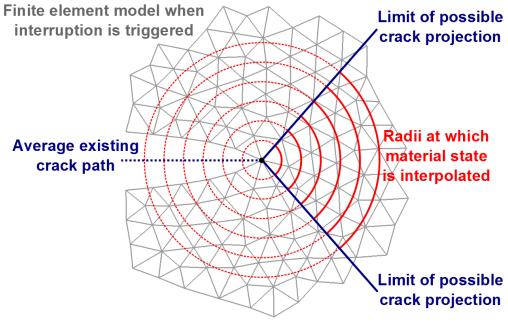

Fig. 2. Schematic display of the key components used in determining the projection of failure in the finite element model

III. METHOD

To test the validity of the iterative procedure presented in Section II-C, two finite element simulations were implemented. The first provided a test of the ability to predict a non-straight crack path. In the second, the procedure was applied to a material with the mechanical properties of a gelatin tissue phantom.

A. Iterative Finite Element Method

In [9] a cohesive zone approach was used to test the development of a crack in a concrete beam. For validation purposes of the iterative procedure, it presents a test of the response to differing combinations of normal and shear loads. This is a vital capability when predicting the response of asymmetric needles and probes. Dimensions and boundary conditions for the concrete beam are shown in Fig. 3. The beam was point loaded in a central position on the top edge and failure was initiated from the tip of a vertical notch, asymmetrically located, on the beam's base.

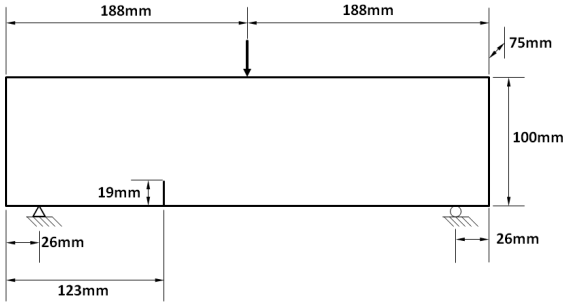

Fig. 3. Configuration of model, based on that used in [9], to generate a combination of shear and normal loading

A plane strain analysis using linear, three-noded elements and an ABAQUS explicit solution procedure was used. The characteristic element length in the area where damage was predicted to occur ranged between 0.7 mm and 1.5 mm in an unstructured mesh. Material constants matched those described in [9] with a Young's modulus, E, of 14.2 GPa, Poisson's ratio, ν, of 0.35. G_c was set to 241 J/m^2. Matlab software controlled the iterative procedure shown in Fig. 1.

B. Iterative Process Applied to a Gelatin Tissue Phantom

Experimental tests were performed on a gelatin tissue phantom material. Blocks 15 mm high, with an 8 mm $\times$ 8 mm section, were stretched by a displacement applied to the top edge while the bottom edge was fixed. Experimentally, the displacement was applied until the block was torn into two sections. A plane strain simulation using the iterative failure procedure was performed to replicate these experiments on the gelatin tissue phantom. An imperfection, triggering failure, was created by a 1 mm horizontal crack at a height of 10 mm as shown in Fig. 4. Following material tests at room temperature, the gelatin was assumed to be rate-independent with $E = 5.2$ kPa, $\nu = 0.45$ and G_c=10 J/m^2.

IV. RESULTS

A. Concrete Beam with Mixed Loading

The failure path that was generated by the iterative algorithm for combined shear and normal loading is shown in Fig. 5. Starting from an asymmetric position, the crack path was initially influenced by shearing and propagated diagonally towards the point of loading. As the failure approached the loading axis, the influence of normal loads became more significant and the trajectory of the failure straightened and approached a vertical direction.

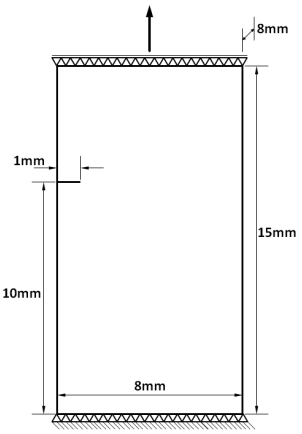

Fig. 4. Model configuration used to represent experimental tensile tests performed on gelatin

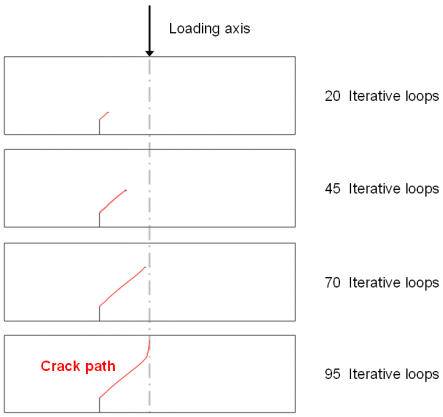

Fig. 5. Progression of the failure path seen in a simulation of a concrete beam subject to a combination of shear and normal stresses

B. Gelatin Tissue Phantom in Tension

In the case of a gelatin tissue phantom subjected to tension on its top face, the failure path was essentially horizontal. Experimentally this is clear as failure progresses in Fig. 6 and results from normal stresses dominating the response. Fig. 7, however, shows the trajectory of failure was not perfectly horizontal for the full sample width. As the point of failure initiation was not on an axis of symmetry, this could be anticipated. Large deformations before failure propagated were also likely to skew the failure path from horizontal.

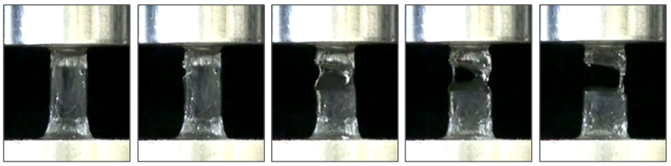

Fig. 6. Crack propagation in an experimental gelatin sample subject to tensile loading

Throughout the simulations, both methods for establishing the projection of failure ((3) and (4)) gave similar results.

Although it is not shown, it was observed that *SED* was more consistent and stable than σ_{norm}. It is not clear whether, under more carefully controlled experimental conditions, the curved crack path seen in the tissue phantom simulation would exist, or whether this is an artefact of poorly tuned constitutive parameters.

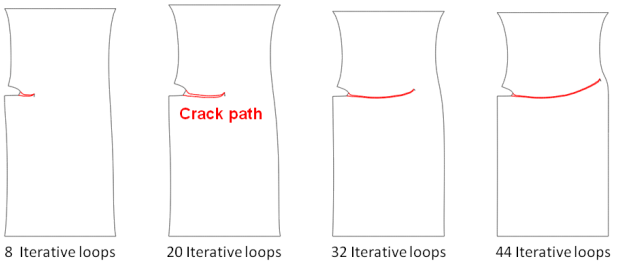

Fig. 7. Failure path that developed in a simulation of tensile loading applied to a gealtin soft tissue phantom

V. DISCUSSION

The results shown in Section IV demonstrate that the iterative finite element approach generated valid failure paths. In response to the conditions outlined in III-A the response correlates with observations in [9] and [13]. There is also a correlation between the horizontal failure of a gelatin sample in Figs. 6 and 7. In this case, the instability and approximate shape of the gelatin renders the sample less than ideal. Due to the large deformations in gelatin, the crack path is also dependent on correct tuning of the trigger stress (Fig. 1) and G_c which is, in turn, temperature and rate dependent in the physical experiments.

Cohesive zone modeling [9] – using a patch with cohesive elements distributed pre-emptively throughout the mesh – and the extended finite element method (XFEM) are alternatives to the iterative procedure used here. However, they lack capabilities for modeling tool-tissue interactions in soft tissue phantoms using commercial software. The iterative procedure eliminates mesh dependency, artificial compliance and difficulties in modeling contact loading seen when implementing cohesive zone techniques. XFEM is extremely effective at modeling crack directions, but is not compatible with surface interactions that generate the failure in tool-tissue interactions.

When using finite elements to optimise the design of a novel tool, e.g. [5], the iterative procedure offers several advantages. Contact loading can be accommodated as readily as if a single predetermined failure path had been specified. With the iterative procedure, the failure path is also determined by the interplay between stress distributions and contact interactions. Considerable insight into optimum bevel angles in a soft tissue phantom, for example, could now be provided using only constitutive model parameters and commercial software.

VI. CONCLUSIONS AND FUTURE WORK

An iterative procedure has been presented that enables the failure of initially continuous finite element models. Using both relatively stiff and soft tissue phantom materials subject to a variety of loading conditions, the predicted failure paths correlate with experimental observations. The finite element models used with the iterative procedure were shown to be both compatible with high resolution simulations and suitable for the optimisation of steerable medical probes.

All numerical results require experimental validation. Consequently the high resolution technique in [14], already applied in a gelatin tissue phantom, will be utilised. This will offer a complete computational and experimental framework to analyse detailed tool-tissue interactions in optimising mechanical performance while limiting tissue trauma. To fully represent physical interactions, constitutive behaviour using large strain material models and biological material parameters will also be implemented.

REFERENCES

[1] S. Misra, K. Reed, B. Schafer, K. Ramesh, and A. Okamura, "Mechanics of flexible needles robotically steered through soft tissue," *The International Journal of Robotics Research*, vol. 29, no. 13, pp. 1640–1660, 2010.

[2] J. A. Engh, D. S. Minhas, D. Kondziolka, and C. N. Riviere, "Percutaneous intracerebral navigation by duty-cycled spinning of flexible bevel-tipped needles," *Neurosurgery*, vol. 67, no. 4, pp. 1117–1123, 2010.

[3] O. Goksel, E. Dehghan, and S. E. Salcudean, "Modeling and simulation of flexible needles," *Medical Engineering & Physics*, vol. 31, no. 9, pp. 1069–1078, 2009.

[4] S. Y. Ko, L. Frasson, and F. Rodriguez y Baena, "Closed-loop planar motion control of a steerable probe with a "programmable bevel" inspired by nature," *Robotics, IEEE Transactions on*, vol. 27, no. 5, pp. 970–983, 2011.

[5] L. Frasson, F. Ferroni, S. Ko, G. Dogangil, and F. Rodriguez y Baena, "Experimental evaluation of a novel steerable probe with a programmable bevel tip inspired by nature," *Journal of Robotic Surgery*, pp. 1–9, 2011.

[6] C. Gokgol, C. Basdogan, and D. Canadinc, "Estimation of fracture toughness of liver tissue: Experiments and validation," *Medical Engineering & Physics*, 2011, doi :10.1016/j.medengphy.2011.09.030.

[7] K. Lister, A. Lau, and J. P. Desai, "Towards a soft-tissue cutting simulator using the cohesive zone approach," in *Engineering in Medicine and Biology Society,EMBC, 2011 Annual International Conference of the IEEE*. IEEE, September 2011, pp. 6691–6694.

[8] G. Geißler, C. Netzker, and M. Kaliske, "Discrete crack path prediction by an adaptive cohesive crack model," *Engineering Fracture Mechanics*, vol. 77, no. 18, pp. 3541–3557, 2010.

[9] S. H. Song, G. H. Paulino, and W. G. Buttlar, "Simulation of crack propagation in asphalt concrete using an intrinsic cohesive zone model," *Journal of Engineering Mechanics*, vol. 132, no. 11, pp. 1215–1223, 2006.

[10] M. Oldfield, D. Dini, G. Giordano, and F. Rodriguez y Baena, "Detailed finite element modelling of deep needle insertions into a soft tissue phantom using a cohesive approach," *Computer Methods in Biomechanics and Biomedical Engineering*, doi: 10.1080/10255842.2011.628448.

[11] ABAQUS, *Abaqus Version 6.9 Documentation*. Providence, RI: Dassault Systemes Simulia Corporation, 2009.

[12] P. O. Bouchard, F. Bay, and Y. Chastel, "Numerical modelling of crack propagation: automatic remeshing and comparison of different criteria," *Computer Methods in Applied Mechanics and Engineering*, vol. 192, no. 35-36, pp. 3887–3908, 2003.

[13] C.-H. Sam, K. D. Papoulia, and S. A. Vavasis, "Obtaining initially rigid cohesive finite element models that are temporally convergent," *Engineering Fracture Mechanics*, vol. 72, no. 14, pp. 2247 – 2267, 2005.

[14] J. Kerl, T. Parittotokkaporn, L. Frasson, M. Oldfield, F. R. y Baena, and F. Beyrau, "Tissue deformation analysis using a laser based digital image correlation technique," *Journal of the Mechanical Behavior of Biomedical Materials*, vol. 6, pp. 159 – 165, 2012.